SUSX-TH-00-010
RHCPP 00-02T
hep-ph/0007206
July 2000

Sparticle spectrum and dark matter in type I string theory with an intermediate scale

D.BAILIN♣ [1], G. V. KRANIOTIS♠ [2] and A. LOVE♠
♣ *Centre for Theoretical Physics,*
University of Sussex,
Brighton BN1 9QJ, U.K.
♠ *Centre for Particle Physics ,*
Royal Holloway and Bedford New College,
University of London,Egham,
Surrey TW20-0EX, U.K.

ABSTRACT

The supersymmetric particle spectrum is calculated in type I string theories formulated as orientifold compactifications of type IIB string theory. A string scale at an intermediate value of $10^{11} - 10^{12}$ GeV is assumed and extra vector-like matter states are introduced to allow unification of gauge coupling constants to occur at this scale. The qualitative features of the spectrum are compared with Calabi-Yau compactification of the weakly coupled heterotic string and with the eleven dimensional supergravity limit of M-theory. Some striking differences are observed. Assuming that the lightest neutralino provides the dark matter in the universe, further constraints on the sparticle spectrum are obtained. Direct detection rates for dark matter are estimated.

[1] D.Bailin@sussex.ac.uk
[2] G.Kraniotis@rhbnc.ac.uk

In a generic supergravity theory, the soft supersymmetry-breaking terms are free parameters. On the other hand, if the supergravity theory is the low energy limit of a string theory, these parameters are calculable in principle in terms of the fewer parameters characteristic of string theory. Once the soft supersymmetry-breaking terms have been determined the renormalization group equations may be run from the string scale to the electroweak scale to derive the sparticle spectrum. Such calculations have been performed in the context of the weakly coupled heterotic string in the large modulus limit of Calabi-Yau compactifications [1], of orbifold compactifications of the weakly coupled heterotic string [1, 2] and of the eleven dimensional supergravity limit of M-theory corresponding to the strongly coupled heterotic string [3, 6]. Here we extend such calculations to scenarios motivated by type I string theories constructed as orientifold compactifications of type IIB string theory [9, 10]. A novel feature of type I theories is that the string scale is a function of the Planck scale and the compactification scale and can, in principle, lie anywhere between about 1TeV and 10^{18}GeV [11]- [15]. A rather natural possibility is for the string scale to be at an intermediate scale of order 10^{11}GeV. Type I theories possess an elegant mechanism for this to occur which may be summarized as follows. It is possible to construct type I theories in which the observable gauge group and quark and lepton matter are associated with 9-branes and 5-branes while supersymmetry is broken directly in non-supersymmetric anti-5-brane sectors. The scale of supersymmetry breaking in the anti-5-brane sector is the type I string scale M_I and the supersymmetry breaking will be transmitted gravitationally to the observable sector. We then expect masses for the supersymmetric particles of order M_I^2/M_P where M_P is the Planck mass. For sparticle masses of order 1TeV we have $M_I \sim 10^{11}$GeV. In a string theory, unification of (tree-level) gauge coupling constants will occur at M_I.

Our purpose here is to study the consequences of such an intermediate string scale for the sparticle spectrum, and for dark matter assuming that the lightest neutralino provides the dark matter in the universe. A novel sparticle spectrum can develop because the renormalization group equations are being run between the electroweak scale and an intermediate scale rather than a scale of order 10^{16}GeV and because unification of gauge coupling constants at M_I may require extra matter (vector-like) between the electroweak scale and M_I. There is some overlap with the work of Abel et al. [16] which appeared in e-print when our work was close to completion. However, we consider some choices of extra matter to achieve intermediate scale unification and some choices of Goldstino angle which differ from these authors and also explore the possibility of an unconventional normalization of the $U(1)$ of the standard model, which is common in type I theories. We also study the implications of the sparticle spectrum in type I theories for dark matter. There is also some overlap with the work of Gabrielli et al [24] which appeared in e-print while we were writting up this work. These authors also considered direct detection rates for neutralino dark matter in theories with intermediate scales.

We shall study two scenarios which illustrate how far the type I sparticle spectrum can differ from the sparticle spectrum obtained in Calabi-Yau compactifications of the weakly coupled heterotic string and from the eleven dimensional supergravity

limit of M-theory corresponding to the strongly coupled heterotic string. In the first scenario (I_a), the additional matter, taken to have mass small on the intermediate scale but large compared to "observable" matter, is taken to be $2L + 3E_R$ vector-like representations, where L is an $SU_L(2)$ lepton-like doublet and E_R is an $SU_L(2)$ singlet with the quantum numbers of the right-handed electron [17]. Unification of gauge coupling constants then occurs at about 10^{11}GeV with the standard normalization $g_1^2/g_2^2 = 3/5$ of the standard model $U(1)_Y$. In the second scenario (I_b), the additional matter is taken to be $6L + 3D_R$ vector-like representations, where D_R is an $SU_L(2)$ singlet and $SU_c(3)$ triplet with the quantum numbers of the right handed d quark. In this case, unification of gauge coupling constants occurs at about 10^{12}GeV with the unconventional normalization of the standard model $U(1)$ $g_1^2/g_2^2 = 3/11$. Scenario I_b is inspired by an explicit Z_3 orientifold model [9] with this latter property, though the model does not have all the properties discussed in the next paragraph.

The soft supersymmetry-breaking terms for type I theories are known where the observable sector gauge group and all observable sector matter are associated with 9-branes, 5-branes or open strings linking 9-branes to 5-branes, and all 5-branes sit at the orbifold fixed point at the origin, so that duality transformations can be exploited to the full. We shall consider the case where there are only 5_i-branes for one value of i, say 5_3-branes, where i labels the complex compact dimension wrapped by the 5-brane, and where there is a single overall modulus T. We shall also assume that the observable gauge group is entirely in the 9-brane sector and the cosmological constant V_0 is zero, so that $C = 1$ in the notation of Brignole et al [1], and that the CP violating phases α_S, α_T are zero. Then, the soft supersymmetry-breaking terms are universal and the same as in the large T limit of the Calabi-Yau compactification of the weakly coupled heterotic string

$$M_{1/2} = \sqrt{3} m_{3/2} \sin\theta \tag{1}$$

$$m_0^2 = m_{3/2}^2 \sin^2\theta \tag{2}$$

$$A = -\sqrt{3} m_{3/2} \sin\theta \tag{3}$$

where $M_{1/2}, m_0$ and A are the observable sector gaugino mass, scalar mass and trilinear scalar coupling, respectively, and $m_{3/2}$ is the gravitino mass. The Goldstino angle θ has been introduced by parametrizing the auxiliary fields F^S and F^T for the dilaton S and modulus T in the form

$$\begin{aligned} F^S &= \sqrt{3} m_{3/2} (S + \bar{S}) \sin\theta, \\ F^i &= \sqrt{3} m_{3/2} (T + \bar{T}) \cos\theta \end{aligned} \tag{4}$$

The effects of twisted sector moduli entering the gauge kinetic function and mixing with the T modulus through a Green-Schwarz term have been neglected.

As mentioned earlier, a novel sparticle spectrum can arise when the renormalization group equations are run from an intermediate string scale of order 10^{11} or 10^{12}GeV instead of 10^{16}GeV, especially when unification at the intermediate scale is

achieved by the introduction of extra matter states, even though the soft supersymmetry-breaking terms at the string scale are not novel. We shall present results for the dilaton dominated case $\theta = \frac{\pi}{2}$ and for a "typical" case $\theta = \frac{\pi}{4}$ but not for $\theta = 0$, in which case the loop corrections become important.

Our parameters are the goldstino angle θ, sign μ (which is not determined by the radiative electroweak symmetry-breaking constraint) [18] where μ is the Higgs mixing parameter in the low energy superpotential and $\tan\beta$, the ratio of Higgs expectation values $\frac{<H_2^0>}{<H_1^0>}$, if we leave B, the coefficient of the soft bilinear term associated with the Higgs mixing term, to be a free parameter to be determined by the minimization of the Higgs potential. Using (1),(2) and (3) as boundary conditions, the renormalization group equations are run from the unification scale to the electroweak scale and the sparticle spectrum is determined consistently with the constraints of correct electroweak symmetry breaking and experimental constraints on sparticle masses from unsuccessful searches at accelerators. The empirical lower bounds we use are $m_{\chi_1^\pm} > 84\text{GeV}$, $m_{\chi_1^0} > 31.6\text{GeV}$, $m_{h_0} > 89.3\text{GeV}$ and $m_{\tilde{g}} > 300\text{GeV}$ [16]. Electroweak symmetry breaking is characterized by the extrema equations

$$\begin{aligned} \frac{1}{2}M_Z^2 &= \frac{\bar{m}_{H_1}^2 - \bar{m}_{H_2}^2 \tan^2\beta}{\tan^2\beta - 1} - \mu^2 \\ -B\mu &= \frac{1}{2}(\bar{m}_{H_1}^2 + \bar{m}_{H_2}^2 + 2\mu^2)\sin 2\beta \end{aligned} \tag{5}$$

where

$$\bar{m}_{H_1,H_2}^2 \equiv m_{H_1,H_2}^2 + \frac{\partial \Delta V}{\partial v_{1,2}^2} \tag{6}$$

and $\Delta V = (64\pi^2)^{-1}\text{STr}M^4[ln(M^2/Q^2) - \frac{3}{2}]$ is the one loop contribution to the Higgs effective potential. Contributions from the third generation of particles and sparticles are included. The chargino mass matrix is

$$M_{ch} = \begin{pmatrix} M_2 & \sqrt{2}m_W \sin\beta \\ m_W \cos\beta & -\mu \end{pmatrix} \tag{7}$$

and the neutralino mass matrix is

$$\begin{pmatrix} M_1 & 0 & -M_Z A_{11} & M_Z A_{21} \\ 0 & M_2 & M_Z A_{12} & -M_Z A_{22} \\ -M_Z A_{11} & M_Z A_{12} & 0 & \mu \\ M_Z A_{21} & -M_Z A_{22} & \mu & 0 \end{pmatrix}$$

with

$$\begin{pmatrix} A_{11} & A_{12} \\ A_{21} & A_{22} \end{pmatrix} = \begin{pmatrix} \sin\theta_W \cos\beta & \cos\theta_W \cos\beta \\ \sin\theta_W \sin\beta & \cos\theta_W \sin\beta \end{pmatrix}$$

also, the stau mass matrix is given by

$$\mathcal{M}_\tau^2 = \begin{pmatrix} \mathcal{M}_{11}^2 & m_{\tilde{\tau}}(A_\tau + \mu \tan\beta) \\ m_{\tilde{\tau}}(A_\tau + \mu \tan\beta) & \mathcal{M}_{22}^2 \end{pmatrix} \tag{8}$$

where $\mathcal{M}_{11}^2 = m_L^2 + m_\tau^2 - \frac{1}{2}(2M_W^2 - M_Z^2)\cos 2\beta$ and $\mathcal{M}_{22}^2 = m_{e_R}^2 + m_\tau^2 + (M_W^2 - M_Z^2)\cos 2\beta$.

We now discuss the qualitative features of the sparticle spectrum for the two scenarios, type I_a and I_b, described earlier and compare with the eleven dimensional supergravity limit of M-theory corresponding to the strongly-coupled heterotic string and with the weakly-coupled heterotic string in the large T limit of Calabi-Yau compactification.

The results of our calculation of the sparticle spectra arising from the different scenarios are presented in Figs.1, 2, 3. For the I_a scenario the sparticle spectra for $\theta = \pi/4$ and $\theta = \pi/2$ differ very little apart from the overall scale which is determined by the gravitino mass. We therefore only present the sparticle spectrum for $\theta = \pi/4$ in I_a scenario. We find also that the choice of sign of μ makes little difference to the spectra. Qualitatively, the principal features are as follows:

- The CP odd Higgs (A^0) is much lighter in the I_a scenario than the I_b. For the most part it is lighter than the lightest stop (st_2) in the I_a scenario, whereas in I_b it is much heavier than (st_2).
- The lightest stau ($s\tau_2$) is also lighter in the I_a scenario than in I_b. In the former it is closer to the lightest chargino (χ_1^+), whereas in the latter it is much heavier than (χ_1^+).
- Moreover, in I_a the (χ_1^+) is much heavier than the lightest neutralino (χ_1^0), whereas in I_b they are almost degenerate, with (χ_1^0) being a few GeV lighter. This has important consequences for dark matter due to coannihilation effects.
- In I_a the gluino is almost the heaviest sparticle, whereas in I_b it is in the middle of the spectrum (and lighter than A_0 for $\tan\beta < 32$).

It is of interest to compare these spectra with those arising in other string scenarios. To allow this comparison we present the sparticle spectra for the extreme M-theory limit in Figs. 4, 5, for the large-T limit of weakly coupled string theory compactified on a Calabi-Yau space Figs. 6, and for the case of mirage unification [19], with soft supersymmetry-breaking terms running from 10^{11}GeV, in Figures 7, 8 (In the case of mirage unification there is no extra matter, so the gauge couplings are *not* unified at the string scale; the "mirage" of unification at 10^{16}GeV is given by string loop effects.). In the extreme M-theory limit case the Goldstino mixing angle $\theta = \frac{\pi}{2}$ is not accessible without the scalar mass squared (m_0^2) becoming negative at the unification scale, hence breaking the electroweak gauge symmetry in models with the standard model gauge group.

The noteworthy qualitative features of this comparison are as follows:

- The I_a spectrum is similar in most respects to that of the extreme M-theory case with $\theta = \frac{\pi}{4}$. However, in the I_a case $s\tau_2$ is heavier than χ_1^+ for $\tan\beta \leq 25$, whereas in the extreme M-theory case it is always lighter than χ_1^+. Furthermore, in the M-theory case, for $\tan\beta > 23$, $(s\tau_2)$ becomes the lightest supersymmetric particle (LSP).

- Most of the foregoing features are insensitive to the Goldstino angle. However, in the extreme M-theory case [3] (see Fig.(5)) with $\theta = \frac{7\pi}{20}$ we have $m_0 \ll M_{1/2}$, the common gaugino mass , whereas for $\theta = \frac{\pi}{4}$ we have $m_0 \sim M_{1/2}$ and this difference produces some qualitative changes. For example, $s\tau_2$ becomes the LSP for $\tan\beta > 9$ when $\theta = \frac{7\pi}{20}$. Also A^0 is now heavier than when $\theta = \frac{\pi}{4}$, and st_2 is lighter than A^0, as is the case in the I_b scenario.

- The spectra deriving from the extreme M-theory limit with $\theta = \pi/4$ (Fig. 4) are similar in most respects to those deriving from the weakly coupled case with $m_{3/2} = 100\text{GeV}$, $\theta = \frac{\pi}{2}$ shown in Fig. 6.

- The spectra arising in the mirage unification scenario (with $\mu > 0$) are similar in most respects to those in I_a. However, for mirage unification $s\tau_2$ is lighter than χ_1^+, whereas it is heavier than χ_1^+ in I_a for $\tan\beta < 25$.

- The spectra arising in the two mirage unification scenarios, $\mu > 0$ and $\mu < 0$, are similar in most respects. However, for $\mu > 0$ χ_1^+ is always heavier than $s\tau_2$, whereas for $\mu < 0$ χ_1^+ is lighter than $s\tau_2$ for $\tan\beta < 17$. Also, for small $\tan\beta$ the masses of A^0 and st_2 are very similar for $\mu > 0$, but very different for $\mu < 0$.

Assuming R-parity conservation the LSP is stable, and consequently if it is neutral can provide a good dark matter candidate. We assume that the dark matter is in the form of neutralinos. The lightest neutralino is a linear combination of the superpartners of the photon, Z^0 and neutral-Higgs bosons,

$$\chi_1^0 = N_{11}\tilde{B} + N_{12}\tilde{W}^3 + N_{13}\tilde{H}_1^0 + N_{14}\tilde{H}_2^0 \tag{9}$$

For both I_a and I_b scenarios the lightest neutralino is the LSP for most of the parameter space and for the mirage unification χ_1^0 is not the LSP only for $\tan\beta > 25$. For these cases one can calculate the resulting relic abundance.

When the observational data on temperature fluctuations, type Ia supernovae, and gravitational lensing are combined with popular cosmological models, the dark matter relic abundance (Ω_{LSP}) typically satisfies [20]

$$0.1 \leq \Omega_{LSP}h^2 \leq 0.4 \tag{10}$$

We calculated the relic abundance of the lightest neutralino in the scenarios we have considered using standard techniques [21]. When these results are confronted with the (model-dependent) bounds (10) derived from the observational data further constraints on the parameters $m_{3/2}, \tan\beta, \mu, \theta$ are obtained and these give new constraints on the sparticle spectrum.

Mass	$\theta = \frac{\pi}{2}, \tan\beta = 10, \mu < 0$	$\theta = \frac{\pi}{2}, \tan\beta = 10, \mu > 0$	$\theta = \frac{\pi}{2}, \tan\beta = 3, \mu > 0$
$m_{3/2}$	113GeV-170GeV	100GeV-167GeV	85GeV-170GeV
$m_{\chi_1^0}$	54GeV-87.5GeV	52.5GeV-89.1GeV	49GeV-93.5GeV
$m_{\chi_1^\pm}$	87GeV-150GeV	88GeV-158GeV	93GeV-174GeV
m_{h^0}	115GeV-123GeV	110GeV-121GeV	89GeV-105GeV

Table 1: Bounds on sparticle masses resulting from Eq. (10.)

Let us start with the I_a scenario. We first present the results of a calculation of the relic abundance for the lightest neutralino as a function of the gravitino mass $m_{3/2}$ for two representative values of $\tan\beta$, $\tan\beta = 3$ and $\tan\beta = 10$. In Fig.9 we plot the relic abundance for the lightest neutralino versus the gravitino mass, $m_{3/2}$, for $\theta = \pi/2$ and $\tan\beta = 3, \mu > 0$. The upper and lower limit (10) on the relic abundance constrain $m_{3/2}$ to lie in the interval $85 \leq m_{3/2} \leq 170$GeV see Table 1..

If instead we take $\tan\beta = 10$, $100\text{GeV} \leq m_{3/2} \leq 167\text{GeV}$ for $\mu > 0$ whereas for $\mu < 0$ $113\text{GeV} \leq m_{3/2} \leq 170\text{GeV}$. In this case one obtains the bounds on the sparticle masses exhibited in Table 1.

The lightest stau for $\mu > 0$ is in the range $114\text{GeV} \leq m_{\tilde{\tau}_2} \leq 185\text{GeV}$. For the same value of $\tan\beta$ the total detection rates for a typical ^{73}Ge detector are in the range $0.07(2\times10^{-2}) - 4.8\times10^{-3}(7\times10^{-4})$events/Kg/Day for $\mu < 0 (> 0)$ respectively. The lightest supersymmetric particle is almost a Bino for both signs of μ. For $\mu < 0$ the Higgsino component is a little bit larger than for $\mu > 0$ but still the LSP is essentially almost a Bino. In Fig. 10 we plot the relic abundance versus $\tan\beta$ for fixed gravitino mass. From this figure we see that for smaller values for the gravitino mass (i.e the lighter the spectrum) $\tan\beta$ is restricted to small values.

In the I_b scenario and for $\mu > 0$ the constraints from (10) have dramatic consequences. As noted earlier there is an almost exact degeneracy of the lightest chargino with the lightest neutralino, $M_{\tilde{\chi}_1^\pm} - M_{\tilde{\chi}_1^0} \leq 3\text{GeV}$. Because of this coannihilation effects [22] become important and the resulting relic abundance is very small. Therefore, if the lightest neutralino (which is almost Wino in this case) makes up most of the non-baryonic dark matter in the universe this model is excluded.

In the mirage unification scenario (without extra matter) cosmological constraints prefer a low $\tan\beta$ and gravitino mass. For instance for $m_{3/2} = 90\text{GeV}$, $\mu < 0$ the relic abundance is in the range $0.12 \geq \Omega_{LSP}h^2 \geq 0.01$ for $3 \leq \tan\beta \leq 8$. In this case, for ^{73}Ge,$^{208}\,Pb$,$^{131}\,Xe$ detectors, detection rates of the neutralinos are in the range of order $10^{-1} - O(1)$events/Kg/day. This illustrates the fact that $\Omega_{LSP}h^2 \sim \frac{10^{-37}cm^2}{<\sigma_{anni}v>}$ and the neutralino annihilation cross section is roughly proportional to the neutralino scattering cross section. Thus as the LSP abundance decreases, its scattering cross section generally increases. For $\Omega_{LSP}h^2 \sim 0.1$ this results in an increased event rate. Thus in this region of the parameter space even if the

neutralino cosmic density is insufficient to close the universe, and other forms of dark matter are needed, the prospects of its direct detection in underground non-baryonic dark matter experiments could be enhanced. This has also been noted by Gabrielli et al [24].

This comparatively large direct detection rate is a consequence of the Higgsino component of the lightest neutralino being comparable to or even larger than the gaugino component. As a result the scalar cross section for the scattering of a neutralino with a nucleon through Higgs exchange increases. The scalar nucleon-LSP cross section is given by [23, 24]

$$\sigma_{scalar}^{(nucleon)} = \frac{8G_F^2}{\pi} M_W^2 m_{red}^2 \left[\frac{G_1(h_0) I_{h_0}}{m_{h_0}^2} + \frac{G_2(H) I_H}{m_H^2} + \cdots \right]^2 \tag{11}$$

where

$$\begin{aligned} G_1(h_0) &= (-N_{11} \tan\theta_W + N_{21})(N_{31} \sin\alpha + N_{41} \cos\alpha) \\ G_2(H) &= (-N_{11} \tan\theta_W + N_{21})(-N_{31} \cos\alpha + N_{41} \sin\alpha) \end{aligned} \tag{12}$$

and

$$I_{h_0,H} = \sum_q l_q^{h_0,H} m_q < N|\bar{q}q|N > \tag{13}$$

and

$$\begin{aligned} l_q^{h_0} &= \frac{\cos\alpha}{\sin\beta} \quad l_q^H = \frac{\sin\alpha}{\sin\beta} \quad \text{for} \quad q = u, c, t \\ l_q^{h_0} &= -\frac{\sin\alpha}{\cos\beta} \quad l_q^H = \frac{\cos\alpha}{\cos\beta} \quad \text{for} \quad q = d, s, b \end{aligned} \tag{14}$$

In equation (11) m_{red} is the neutralino-nucleon reduced mass, h_0, H denote the lightest Higgs and CP-even heavier Higgs respectively and α is the Higgs mixing angle. We note also the $\tan\beta$ dependence of the scalar neutralino-nucleon cross section $\sigma_{scalar}^{nucleon}$. For high values of $\tan\beta$ the corresponding cross section generically increases. The ellipsis denotes the contribution to the scalar cross-section through squark exchange which we have not written explicitly, although we included it in the calculations [3]. We note that, even if the scalar (spin-independent) interaction is the dominant one, the spin-dependent interaction through Z-exchange is also appreciable in this case since it is proportional to the difference $[|N_{31}|^2 - |N_{41}|]^2$ [3].

In summary, the three intermediate scale scenarios studied have sparticle spectra with striking qualitative features which distinguish them from each other and from the M-theory and weakly coupled heterotic string cases. Moreover, the composition of the lightest neutralino differs in the three scenarios. (It is almost Wino for the I_b scenario, with a large Higgsino component for the mirage unification scenario, and almost Bino for the I_a scenario, as well as for the M-theory and weakly-coupled heterotic string cases.) If we assume that the lightest neutralino provides the dark matter in the universe, constraints on the relic abundance put lower and upper bounds on

the sparticle masses in each scenario. Also, the I_b scenario is then excluded because coannihilation effects result in a too small relic abundance. Direct detection rates for the lightest neutralino in the I_a scenario are similar to those for M-theory and weakly coupled heterotic string models. Interestingly, direct detection rates one or two orders of magnitude larger are obtained in the mirage unification scenario where the lightest neutralino has a large Higgsino component.

Acknowledgements

This research is supported in part by PPARC.

References

[1] A. Brignole, L.E. Ibáñez and C. Muñoz, Nucl. Phys.B422(1994)125

[2] B. de Carlos, J. A. Casas and C. Muñoz, Phys. Lett.B 299(1993); G.V. Kraniotis, Z. Phys.C71(1996)163; S. Khalil, A. Masiero and F. Vissani, Phys. Lett.B375(1996)154; A. Love and P. Stadler, Nucl.Phys.B515(1998)34

[3] D. Bailin, G.V. Kraniotis and A. Love, Phys.Lett.B432(1998)90; Nucl.Phys.B556(1999)23;Phys.Lett.B463(1999)174

[4] C.E. Huang, T. Liao, Q. Yan and T. Li, hep-ph/9810412

[5] J.A. Casas, A. Ibarra and C. Munoz,hep-ph/9810266

[6] D.C. Cerdeno and C. Munoz, hep-ph/9904444

[7] T. Li, MADPH-99-1109, hep-ph/9903371

[8] T. Kobayashi, J. Kubo and H. Shimabukuro, HIP-1999-14/TH, hep-ph/9904201

[9] G. Aldazabal, L. E. Ibáñez, F. Quevedo, hep-th/9909172 JHEP 0001 (2000)031

[10] G. Aldazabal, .E. Ibáñez, F. Quevedo and A. Uranga, hep-th/0005067

[11] E. Witten, Nucl. Phys. B471(1996)135

[12] J.D. Lykken, Phys.Rev.D 54 (1996)3693

[13] N. Arkani-Hamed, S. Dimopoulos, G. Dvali, Phys.Lett.B429(1998) 263

[14] I. Antoniadis, N. Arkani-Hamed, S. Dimopoulos, G. Dvali, Phys.Lett.B 436(1998)257

[15] K. Benakli, Phys.Rev.D60(1999):104002

[16] S.A. Abel, B. C. Allanach, F. Quevedo, L.E. Ibáñez and M. Klein, hep-ph/0005260

[17] C.P. Burgess, L.E. Ibáñez and F. Quevedo, Phys.Lett.B447(257)1999, hep-ph/9810535

[18] L. Ibanez, G.G. Ross: Phys. Lett. B110 (1982) 215; L. Alvarez-Gaume, J. Polchinsky and M. Wise: Nucl. Phys. B221 (1983) 495; J. Ellis, J.S. Hagelin, D.V. Nanopoulos and K. Tamvakis: Phys. Lett. B125 (1983) 275; M. Claudson, L. Hall and I. Hinchliffe: Nucl. Phys. B228 (1983) 501; C. Kounnas, A.B. Lahanas, D.V. Nanopoulos and M. Quiros: Nucl. Phys. B236 (1984) 438; L.E. Ibáñez and C. Lopez: Nucl. Phys. B233 (1984) 511; A. Bouquet, J. Kaplan, C.A. Savoy: Nucl. Phys. B262 (1985) 299

[19] L. E. Ibáñez, hep-ph/9905349

[20] N. Bahcall, J.P. Ostriker, S. Perlmutter and P.J. Steinhardt Science 284(1999)1481

[21] G. Jungman, M. Kamionkowski and K. Griest, Phys. Rep.267(1996)195

[22] S. Mizuta and M. Yamaguchi, Phys.Lett.B298(1993)120

[23] D. Bailin, G. V. Kraniotis and A. Love, Nucl.Phys.B556 (1999)23 and references therein

[24] A. Bottino, F. Donato, N. Fornengo, S. Scopel, hep-ph/9909228;J. Ellis, A. Ferstl and K. Olive hep-ph/0007113; E. Accomando, R. Arnowitt, B. Dutta and Y. Santoso, hep-ph/0001019; E. Gabrielli, S. Khalil, C. Muñoz and E. Torrente-Lujan, hep-ph/0006266

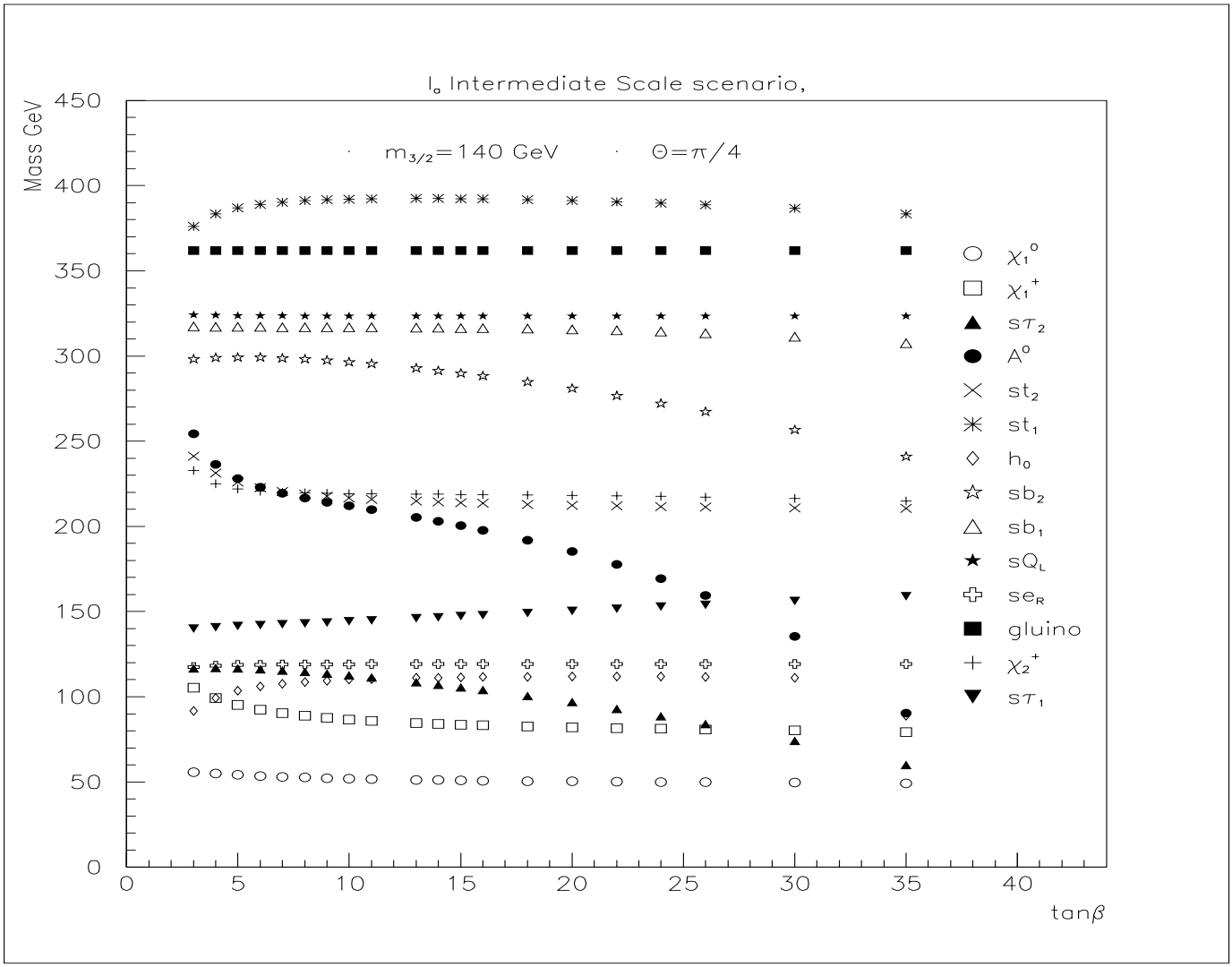

Figure 1: I_a scenario sparticle spectrum vs $\tan\beta$ for $m_{3/2} = 140GeV, \mu > 0, \theta = \pi/4$

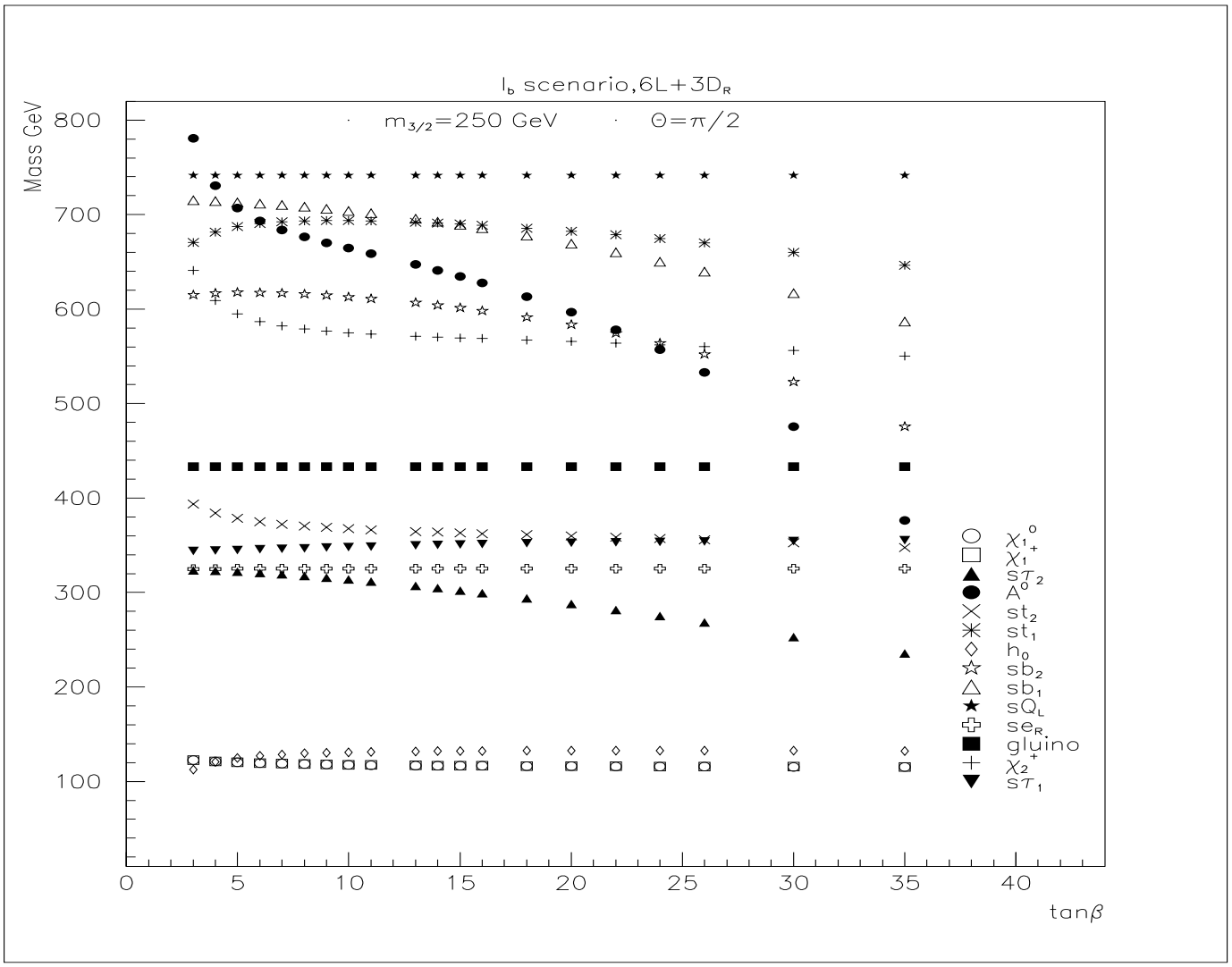

Figure 2: Sparticle spectrum vs $\tan\beta$ I_b scenario with $6L+3D_R$, $m_{3/2} = 250GeV, \mu > 0, \theta = \pi/2$

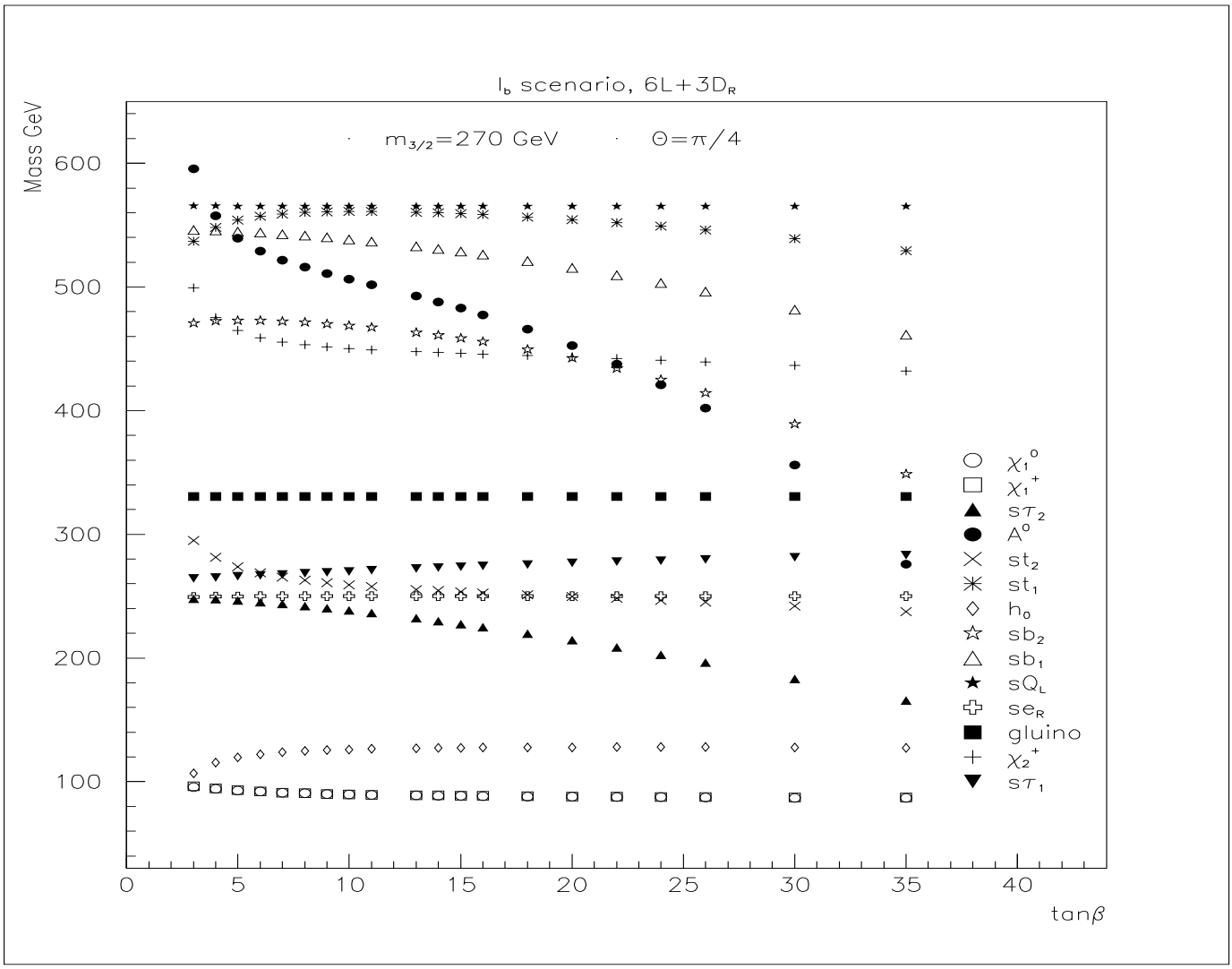

Figure 3: Sparticle spectrum vs tan β I_b scenario with $6L+3D_R$, $m_{3/2} = 270GeV, \mu > 0, \theta = \pi/4$

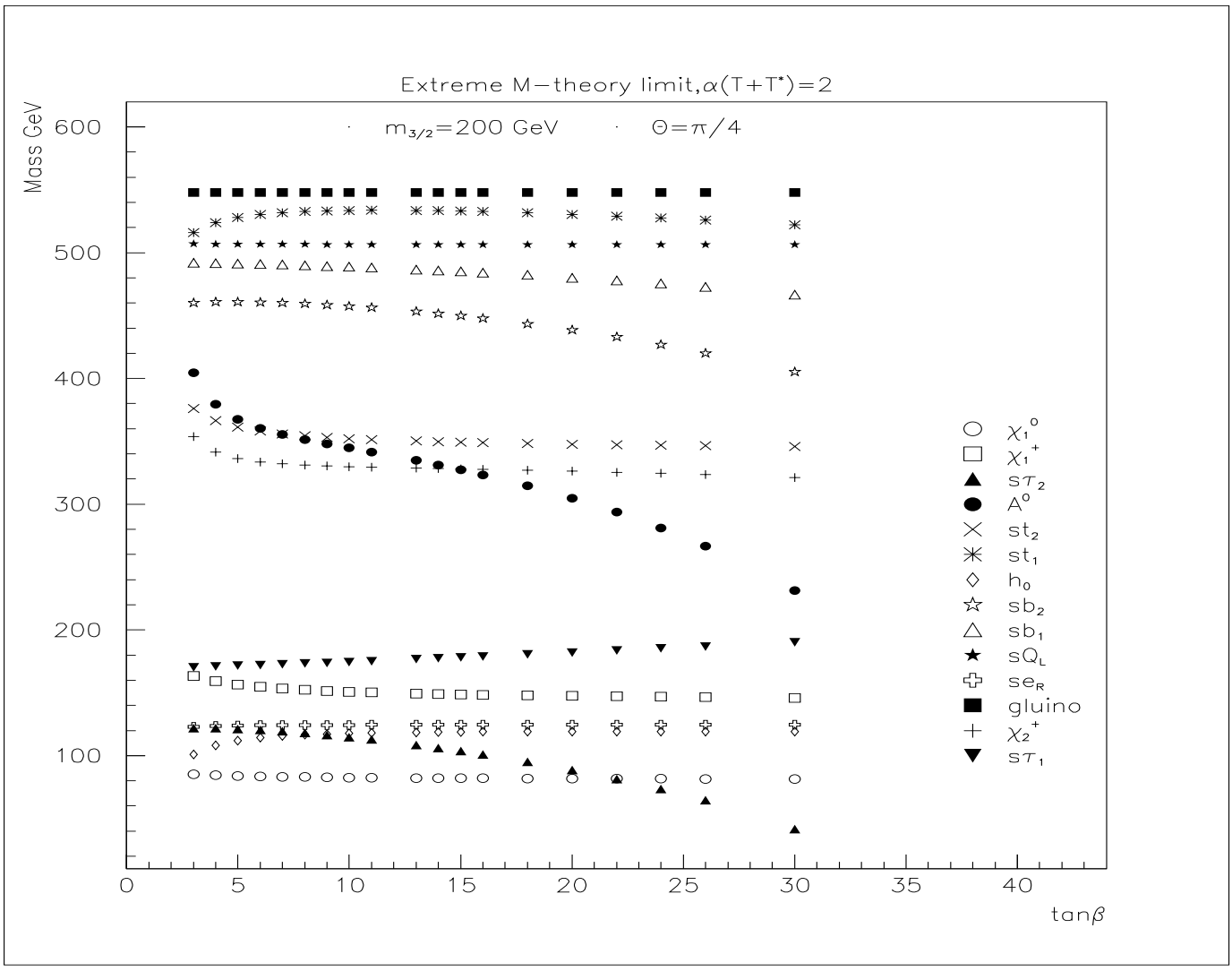

Figure 4: Sparticle spectrum vs $\tan\beta$ in extreme M-theory limit, i.e $\alpha(T+\bar{T})=2$, $\theta=\frac{\pi}{4}$, $m_{3/2}=200GeV, \mu>0$.

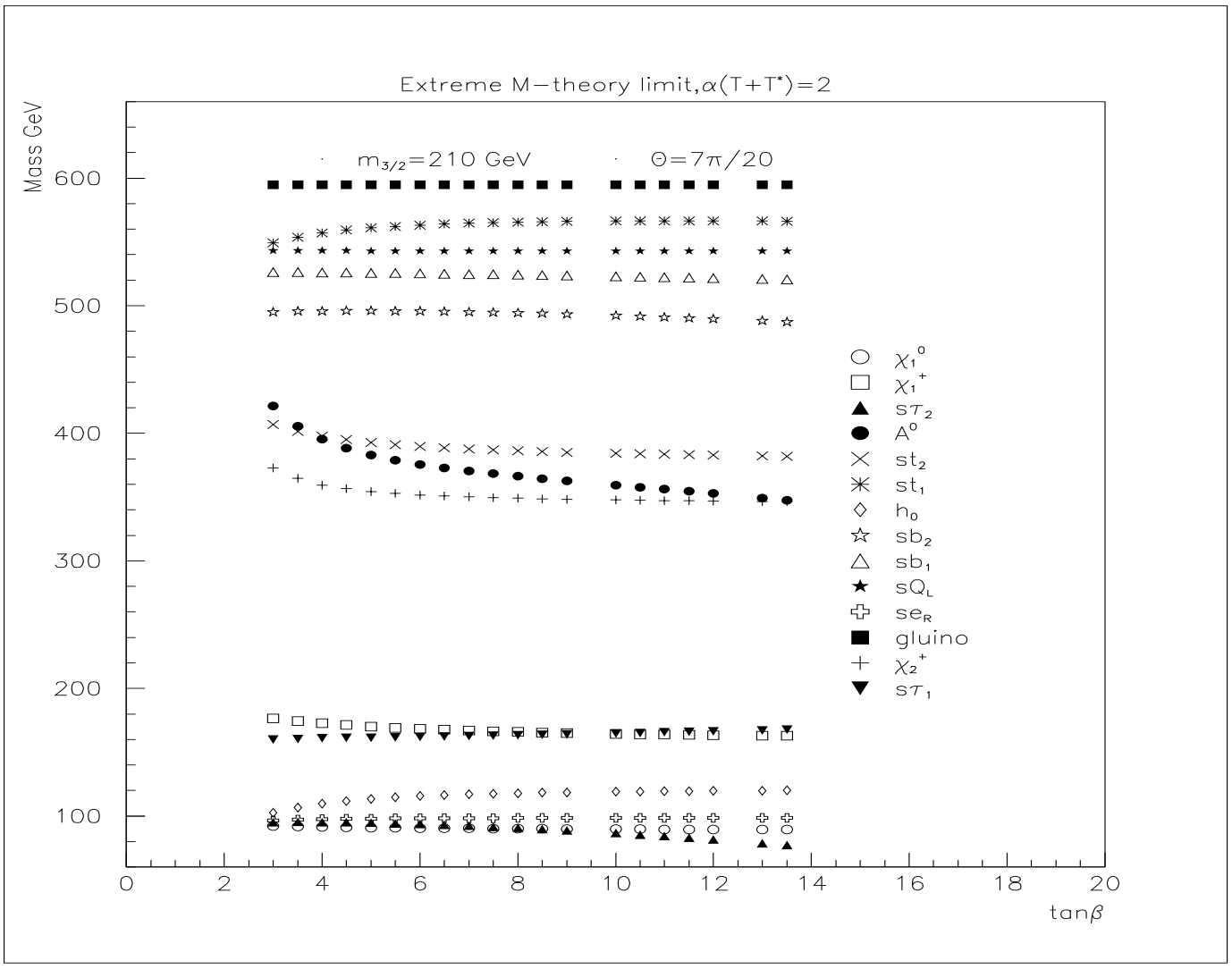

Figure 5: Sparticle spectrum vs $\tan\beta$ in extreme M-theory limit, i.e $\alpha(T+\bar{T})=2$, $m_{3/2}=210GeV$, $\theta=\frac{7\pi}{20}$, $\mu>0$.

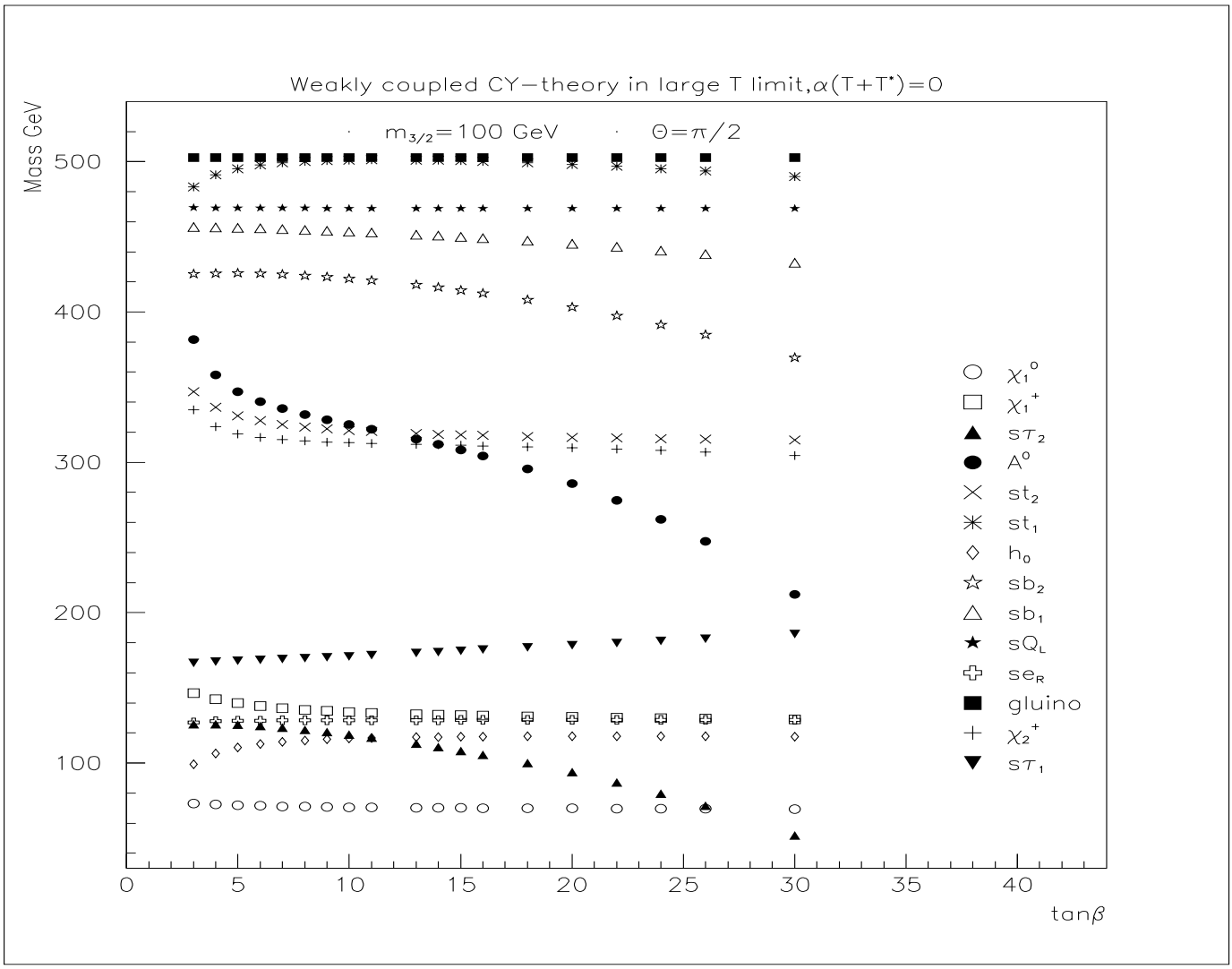

Figure 6: Sparticle spectrum vs $\tan\beta$, $m_{3/2} = 100GeV, \mu > 0$, in the large T-limit of weakly-coupled CY space, $\theta = \pi/2$

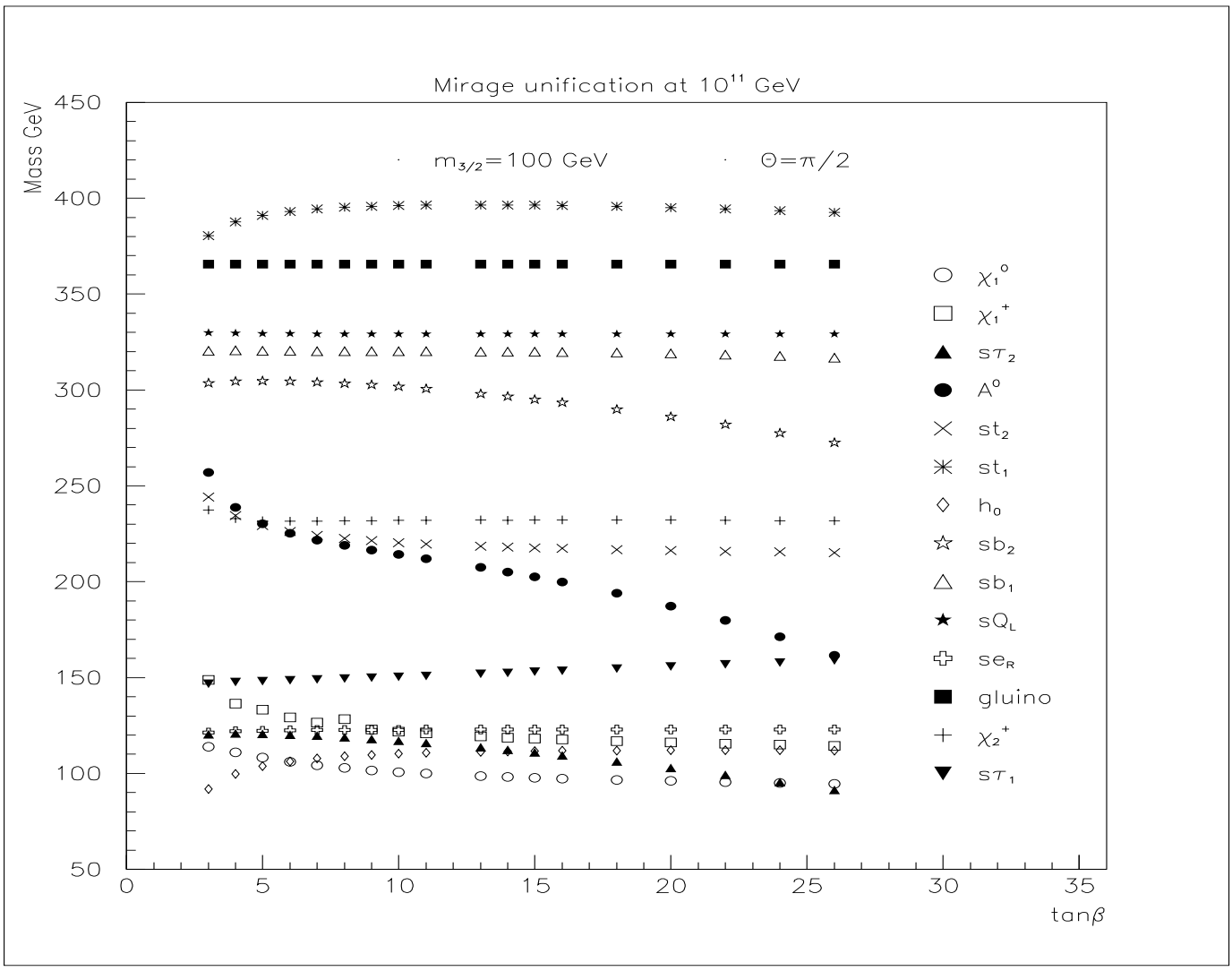

Figure 7: Sparticle spectrum vs $\tan\beta$, in mirage unification scenario, $m_{3/2} = 100GeV, \mu > 0$.

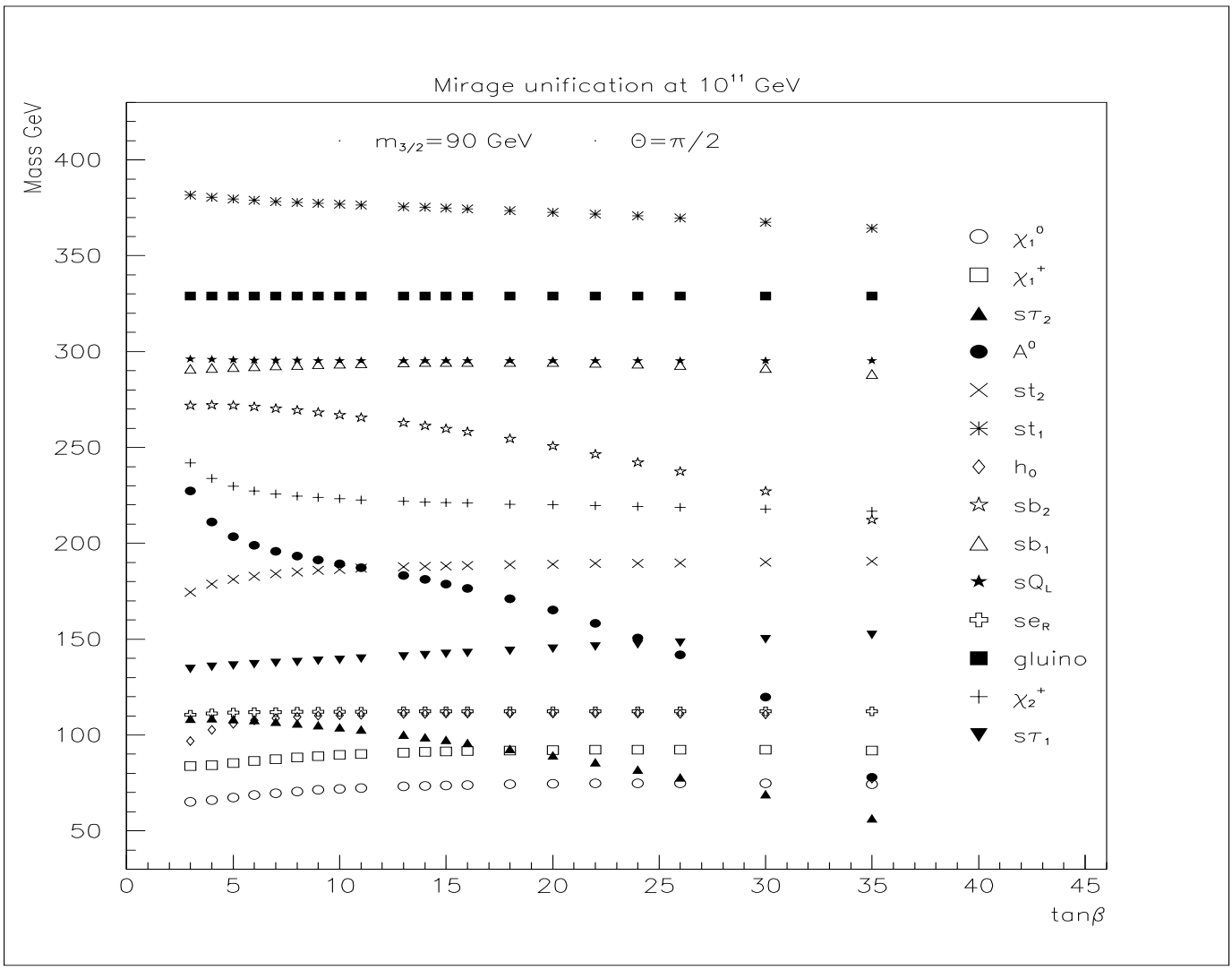

Figure 8: Sparticle spectrum vs $\tan\beta$ in mirage unification scenario, $m_{3/2} = 90GeV, \mu < 0$.

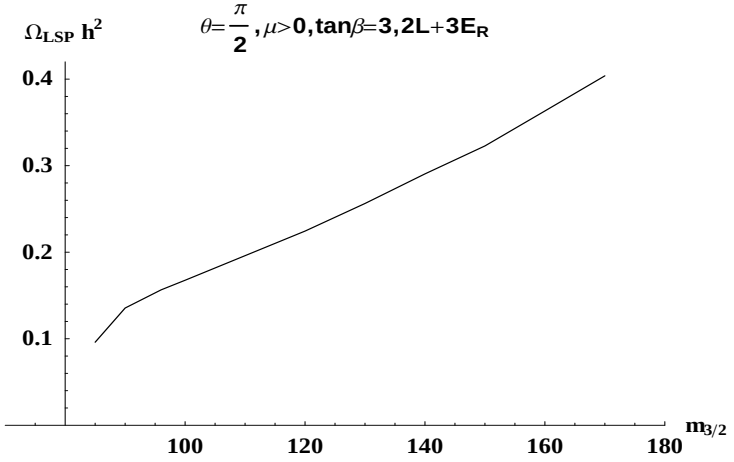

Figure 9: Relic abundance of LSP vs $m_{3/2}$, I_a scenario with $2L + 3E_R$, $\tan\beta = 3, \mu > 0, \theta = \pi/2$

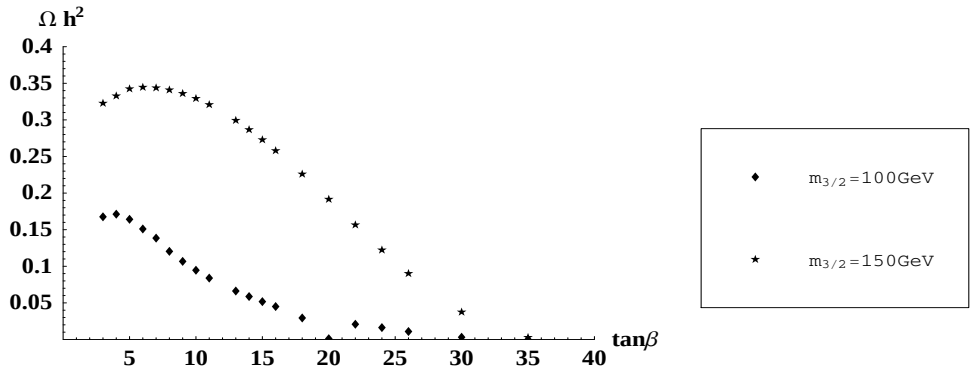

Figure 10: Relic abundance of LSP vs $\tan\beta$, I_a scenario with $2L + 3E_R$, $m_{3/2} = 100, 150\text{GeV}$, $\mu > 0, \theta = \pi/2$